Comparison of registered paper surface representations from microtomography and photometric stereo

MARJA METTÄNEN[1], MATTI JUKOLA[1], ARTTU MIETTINEN[2], HEIMO IHALAINEN[1], TUOMAS TURPEINEN[2], JUSSI TIMONEN[2]

[1]Department of Automation Science and Engineering / Tampere University of Technology
P.O.Box 692, 33101 Tampere, Finland
[2]Department of Physics / University of Jyväskylä
P.O.Box 35 (YFL), 40014 University of Jyväskylä, Finland
marja.mettanen@tut.fi

Keywords: surface topography, photometric stereo, X-ray microtomography

ABSTRACT

Paper and cardboard samples have been imaged with a laboratory-scale photometric stereo device with a spatial resolution of approximately 7 µm and by an X-ray microtomograph with resolutions of 7.1 µm, 3.8 µm and 1.4 µm. The photometric stereo based surface gradients and topography maps are compared with the surface representations that have been estimated from the three-dimensional microtomography data. The correspondence of the spatially aligned surface reconstructions is evaluated through pointwise correlation and 2D coherence that reveals the scales at which the surface roughness is similar in two topography maps. The estimates of the orientation distribution of the topographic features are also compared.

1 INTRODUCTION

Photometric stereo is a fast non-contact solution to acquiring surface topography maps of paper samples [1]. To estimate surface topography by photometric stereo, the sample is first imaged with a camera using slanting illumination from at least two directions. Then the gradients of the surface are computed from the images, and finally the surface topography is estimated from the gradients by integration that involves noise removal and compensation of the point spread function. The method has been used successfully in relating missing ink with the depressions on the paper and cardboard surfaces [1,2,3]. The on-line applicability of the method also motivates to further investigate the practical limitations and possibilities of this image based measurement to characterize paper surface, e.g., in terms of roughness and fibre orientation.

The problem with the photometric stereo method in the measurement of paper stems from the violation of the assumptions regarding the behaviour of light on the surface of the examined material. Paper does not exactly have a Lambertian surface in the micrometre scale, and light is occasionally reflected from the internal fibre surfaces [4]. In addition, erroneous surface height estimates may occur at points of specular reflection, or at steep and deep pores on the paper surface that are unreachable by light [5,6]. The surface representation also depends on the parameter values chosen at the integration stage. The present work is aimed at comparing the photometric stereo (PS) based surface topography reconstructions of paper and cardboard samples with ones obtained through X-ray microtomography that is considered as the reference measurement.

X-ray microtomography (X-µCT) is a non-destructive method for obtaining the three-dimensional (3D) structure of a physical sample [7]. Historically the method has been available in synchrotron X-ray facilities only, but during last years, laboratory-scale devices with resolution adequate for material characterisation have become available.

The method is based on taking a series of two-dimensional (2D) X-ray projection images at a multitude of angles around the sample. A three-dimensional map of X-ray attenuation coefficients is reconstructed computationally from the 2D projection data. The attenuation coefficients distinguish different materials from each other such that their map can be treated as a three-dimensional image of the structure of the sample. A recent review of theoretical and practical structural analysis of paper using 3D tomography has been presented by Bloch and Rolland du Roscoat [8].

Surface topography maps are estimated from the 3D microtomography data by an iterative computational method referred to as the "carpet" method. It is based on the Edwards-Wilkinson equation [9] which is well known in the physics of dynamic interfaces under the influence of random forces. The carpet method has been used previously, for instance, to detect the local structures of base paper and coating layer [10].

In the current work, the surface reconstructions made of the 3D microtomography data are registered and compared with the PS based topography maps. The correspondences of the surface reconstructions are evaluated through statistical methods such as 2D squared coherence. The orientation distributions of the surface topography estimates are also compared. The long term goal of the analyses is to answer two questions. First, is it possible to optimize the photometric stereo based surface topography estimate by adjusting the illumination conditions and the integration parameters? Second, how reliably can the orientation of the surface fibres be

estimated from the images related to the photometric stereo method?

This paper is organized as follows. Section 2 introduces the measured samples and data acquisition. Section 3 describes the surface reconstruction and image registration. The comparisons of the surface representations are described in Section 4, and Section 5 concludes the work.

2 MEASUREMENT DATA

The material studied in this work contains six samples divided into two groups. The first group contains three paper samples that have been imaged from an area of 10 × 10 mm^2 with both the camera system and the X-ray microtomograph. The second group consists of two paper samples and one uncoated cardboard sample. Two separate measurement areas have been marked on each of these samples, and each area has been imaged with the microtomograph using two different resolutions, and with the camera system using a fixed resolution. Table 1 presents a summary of the acquired data.

Photometric stereo images have been taken on each of the nine measurement areas and both sides of each paper/cardboard sample. These images cover an area of 32.5 × 21.5 mm^2 except for paper samples 1-3 (see Table 1) for which the area is 10 × 10 mm^2. In the purpose-built photometric stereo imaging setup, the illumination has been implemented by four white led lights attached at increasing heights to an arm that is rotated around the sample. The system provides, for each sample, 672 images, comprising of 168 illumination angles around the sample and four illumination angles with respect to the surface normal: 82º, 73º, 59º and 46º. The surface gradients are estimated from the images by a least squares method.

The X-µCT measurement has been performed with the SkyScan 1172 device employing cone-beam geometry that allows easy tuning of image resolution. Hence, two image pixel sizes, 7.1 µm and 1.4 µm, have been used for samples 4-6 (see Table 1). The tomography scans have been performed in the absorption contrast mode using 50 kV X-ray tube voltage and 0.3 degree angular step size. The reconstruction has been done with the SkyScan's NRecon software employing standard corrections for temperature drift and rotation axis misalignment.

It is worth noting that the voxels in the X-µCT data have the same size in all three directions (x,y,z), so the resolution directly affects the size of the imaged area. The data sets with a resolution of 1.4 µm thus present an area as small as 5.0 mm by 2.7 mm. Figure 1 exemplifies the various sizes of imaged areas in the case of samples 4, 5, and 6.

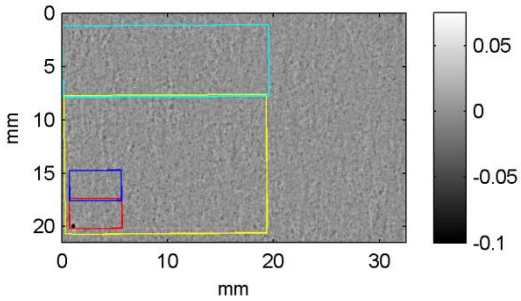

Figure 1. One of the two imaged areas of the cardboard sample. The grayscale image is the PS based topography map, the colorbar signifies the surface heights as millimeters, and the rectangles represent the X-µCT measurement areas: yellow and cyan for 7.1 µm resolution and red and blue for 1.4 µm resolution.

3 SURFACE RECONSTRUCTION AND REGISTRATION

One of the challenges in this work is the detection of the paper surface from the 3D X-µCT data. The current approach is based on the "carpet" method, where the surface is defined as a propagating interface obeying the Edwards-Wilkinson equation [11]. Let the height of the surface above the paper be h and its initial value h_0. The surface is defined by determining the static solution of

$$\begin{cases} \dfrac{\partial h}{\partial t} = \vartheta \nabla^2 h + V + \eta \\ h(t=0) = h_0, \end{cases}$$

where ϑ controls surface tension, V is constant pushing the surface towards the paper and η is the scaled gray value from the image. The carpet method is applied to each of the 3D tomography data arrays to reconstruct the surface topography maps of both the top and bottom side of the paper.

The surface topography maps reconstructed from the microtomography data are registered with the

Table 1. Summary of measurements.

Sample	X-µCT measurement area	X-µCT resolution	PS measurement area	PS resolution	Remarks
paper 1	10 mm × 10 mm	3.7 µm	10 mm × 10 mm	6 µm	one test area per sample
paper 2	10 mm × 10 mm	3.8 µm	10 mm × 10 mm	6 µm	one test area per sample
paper 3	10 mm × 10 mm	3.8 µm	10 mm × 10 mm	6 µm	one test area per sample
paper 4	5.0 mm × 2.7 mm 20 mm × 13 mm	1.4 µm 7.1 µm	32.5 mm × 21.5 mm	7.5 µm	two test areas per sample
paper 5	5.0 mm × 2.7 mm 20 mm × 13 mm	1.4 µm 7.1 µm	32.5 mm × 21.5 mm	7.5 µm	two test areas per sample
cardboard	5.0 mm × 2.7 mm 20 mm × 13 mm	1.4 µm 7.1 µm	32.5 mm × 21.5 mm	7.5 µm	two test areas per sample

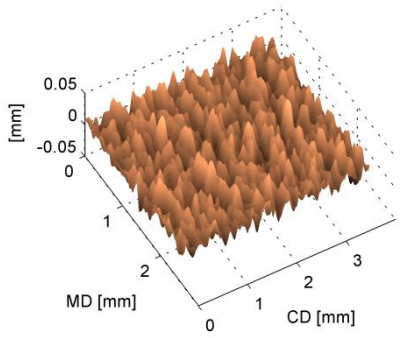

(a) Photometric stereo (spatial resolution 7.5 µm)

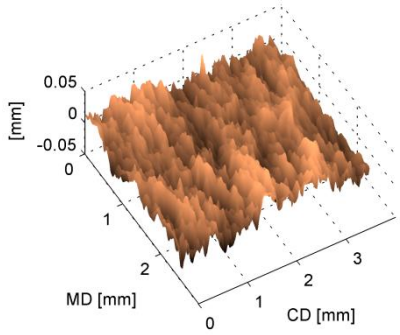

(b) Microtomography (7.1 µm per pixel)

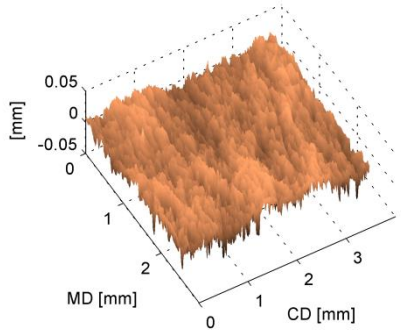

(c) Microtomography (1.4 µm per pixel)

Figure 2. Surface of the bottom side of the uncoated cardboard sample on a 3.8 mm by 2.6 mm area reconstructed from (a) PS images with all illumination angles combined, (b, c) X-µCT data of resolution 7.1 µm and 1.4 µm, respectively.

PS based surface topography maps. The surface representations, exemplified in Figure 2, often exhibit similar features that enable the detection of matching points based on cross-correlation. An affine transformation between the maps is estimated from a few hundred matching point pairs.

4 ANALYSIS AND RESULTS

Once the spatial transformation between two surface representations has been found, the images are aligned. The affine transformation is applied to the coordinates of the PS based topography map, and the pixel values of the tomography based map are interpolated to these new coordinates. The pointwise correlation coefficient between the aligned maps is typically between 0.5 and 0.7.

Coherence reveals the wavelength-dependent correspondence between the surface topography maps estimated with the different methods [12]. Coherence has been estimated pairwise between the three surface topography maps: the one based on photometric stereo and the ones based on X-µCT with resolutions of 7.1 µm and 1.4 µm. Figure 3 shows the 2D spectra of the maps presented in Figure 2(a) and 2(c), and their 2D squared coherence. The frequencies below which the coherence is high are interpreted as the limits of the scale at which the surface roughness is similar in the PS based and the tomography based topography maps. In Figure 3(c), the squared coherence is higher than 0.5 (i.e., correlation coefficient > 0.7) at frequencies below approximately 10 mm^{-1} in the cross direction (CD) and 7 mm^{-1} in the machine direction (MD), which correspond to wavelengths

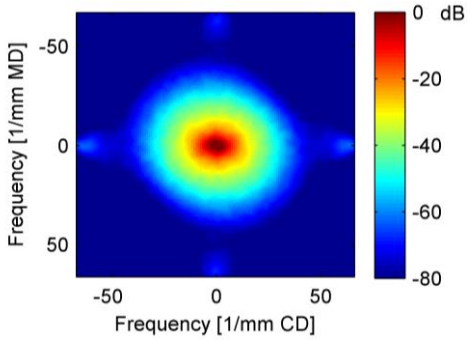

(a) Spectrum of the PS based topography map.

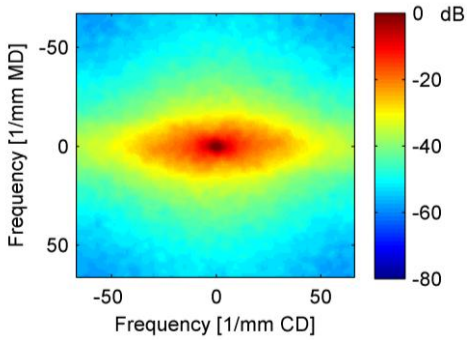

(b) Spectrum of the X-µCT based topography map.

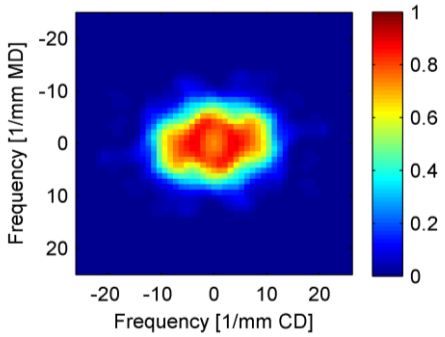

(c) Squared coherence.

Figure 3. 2D power spectra of (a) the photometric stereo based topography map (Fig. 2(a)) and (b) the tomography based surface topography map of resolution 1.4 µm (Fig. 2(c)). (c) Squared 2D coherence between the maps.

Table 2. CD and MD ([*x*, *y*]) wavelength (λ) limits below which the squared coherence falls below 0.5, using the specified illumination angles in the PS based surface topography estimation.

Illumination angle	λ limits [*x*, *y*], PS vs. 7.1 µm	λ limits [*x*, *y*], PS vs. 1.4 µm
82º	[128, 175] µm	[101, 137] µm
73º	[113, 175] µm	[96, 137] µm
59º	[113, 160] µm	[96, 137] µm
46º	[113, 175] µm	[96, 148] µm

longer than around 96 µm and 137 µm, respectively. The coarser resolution (7.1 µm) tomography based surface estimate has higher than 0.5 squared coherence with the PS based map at wavelengths longer than 113 µm in CD and 175 µm in MD. These results apply for the topography map that has been estimated by the photometric stereo method using the combination of all four illumination angles (with respect to the surface normal). Table 2 presents the corresponding results for the PS based topography maps computed with one illumination angle at a time.

The coherence behaviour described above is typical of the samples imaged for this study. The results show only slight dependence on the light configuration used in photometric stereo imaging. The similarity of the surface roughness scales is, however, dependent on the methods of estimating the surface heights from the X-µCT data and from the photometric stereo images. Further experiments are required to see if the correspondence between the surface topography estimates can be enhanced at wavelengths closer to the width of fibres.

While image alignment is a prerequisite for the joint statistical analysis of the multivariate surface height maps, it forces the maps into the same spatial resolution and may thus lose some of the details of the tomography based surface representations. The interpolation of the pixel values is thus omitted in the orientation analysis, and the same area is just selected from each map based on the correspondence of the spatial coordinates that has been discovered in the image registration phase. The orientation of the paper surface structure is estimated from the x- and y-gradients. They are computed from the tomography based surface representations by convolution with a gradient operator. In the case of the photometric stereo method, the x- and y-gradients are readily available as they have been estimated from the images taken with the camera. Surface orientation is described by the surface orientation distribution, and it can be summarized by circular statistics [13]. Figure 4 presents the orientation distributions estimated from the map shown in Figure 2(a) and from the corresponding areas of the X-µCT based topography maps. Each map has been band-pass filtered with limit wavelengths of 50 µm and 200 µm before the orientation analysis. The solid lines describe the distribution of variance with

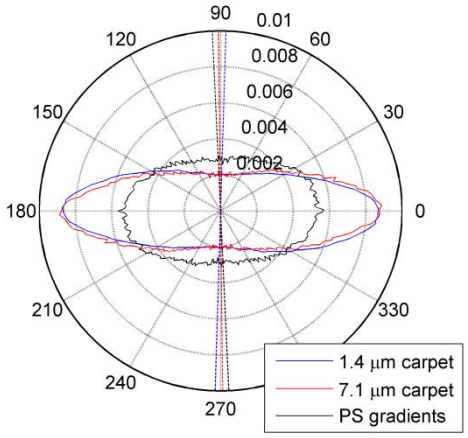

Figure 4. Orientation estimates from the cardboard surface topography maps shown in Figure 2. The solid lines represent the orientation distributions and the straight dashed lines show the main orientation direction relative to the cross direction.

respect to direction. The main orientation of the surface structures is thus perpendicular to the main axis of the ellipse.

The estimated main orientation directions relative to MD are -1.7º, 0.7º and 2.6º for the 1.4 µm and 7.1 µm carpet estimates and the PS based topography estimate, respectively. Similar discrepancies have been found with other analysis areas. The respective circular variances of the orientation distributions are 0.65, 0.66 and 0.84, which are rather high. The theoretical maximum of circular variance is 1.0 and it corresponds to a distribution with no single preferred orientation direction. The results reflect the fact that the area used for the orientation estimation is small and contains only a small number of fibres or other oriented features.

Despite the uncertainty of the surface orientation estimates, the work done so far is a good start to the effort towards our long term goals. The success of the image registration opens up the possibility of aligning the 2D and 3D data. Eventually the purpose is to compare the orientation distribution estimated from the photometric stereo images or gradients to the orientation of the surface fibres that can be determined from the reference X-µCT data. The assumption is that the orientation of the surface structures, particularly in the appropriate size scale, is related to the orientation of the surface fibres. Versatile experiments on the illumination and other details of the photometric stereo method can also be made with the purpose-built laboratory setup. For on-line applications, it is of particular interest to characterize the paper surface based on the gradient information without the integration of the surface.

5 CONCLUSIONS

The goal of this work was to assess the capability of the camera based approach of producing correct description of the paper surface. The topography

maps estimated from the camera based images were successfully registered with those estimated from the X-µCT data, and 2D coherence analysis revealed that the various topography maps present similar surface roughness on wavelengths longer than approximately 100...160 µm, depending on direction and resolution. The orientation distributions were computed from surface topography maps that had been estimated from the data of the two separate measurement devices but presented exactly the same area in different resolutions. As the variance of the orientation distributions was rather high, the main orientation direction of the topographic structures was considered similar in the compared maps.

The analysis of the valuable data set presented in this paper will continue in the near future. The next major step will be the comparison of the whole 3D X-µCT image of the sample with the photometric stereo based 2D surface topography estimate. The current work applied the carpet method for the estimation of the surface topography map from the X-µCT data, but it was not optimized for the detection of the surface fibres. The future work will focus more on the fibres in order to obtain a reliable surface fibre orientation reference. We will investigate the possibility of estimating the surface topography from the 3D tomography data so that not only the original X-ray absorbance values but also their local variance in the (x,y)-plane affect the detection of the surface.

REFERENCES

[1] P. Hansson and P.-Å. Johansson. Topography and reflectance analysis of paper surfaces using a photometric stereo method. *Optical Engineering* **39**(9):2555–2561 (2000).

[2] G.G. Barros and P.-Å. Johansson. Prediction of UnCovered Area occurrence in flexography based on topography – A feasibility study. *Nordic Pulp & Paper Res. J.* **21**(2):172-179 (2006).

[3] M. Mettänen. Measurement of print quality: Joint statistical analysis of paper topography and print defects. PhD thesis, Tampere University of Technology (2010).

[4] G. Chinga. Detailed paper surface characterization for gloss assessment. *J. Pulp Paper Sci.* **30**(8):222-227 (2004).

[5] G.G. Barros and P.-Å. Johansson. The OptiTopo technique for fast assessment of paper topography – Limitations, applications and improvements. *J. Imaging Sci. Tech.* **49**(2):170-178 (2005).

[6] T. Kuparinen. Reconstruction and analysis of surface variation using photometric stereo. PhD thesis, Lappeenranta University of Technology (2008).

[7] A.C. Kak and M. Slaney. Principles of Computerized Tomographic Imaging. IEEE Press (1988).

[8] J.-F. Bloch and S. Rolland du Roscoat. Three-dimensional structural analysis. Advances in Pulp and Paper Research, Trans. 14th Fund. Res. Symp. (S.J. I'Anson, ed.), Oxford, FRC, 599-664 (2009).

[9] S.F. Edwards and D.R. Wilkinson. The surface statistics of a granular aggregate. *Proc. Roy. Soc. (Lond.) A* **381**:17-31 (1982).

[10] G. Chinga-Carrasco, H. Kauko, M. Myllys, J. Timonen, B. Wang, M. Zhou and J.O. Fossum. New advances in the 3D characterization of mineral coating layers on paper. *J. Microscopy* **232**(2):212-224 (2008).

[11] T. Turpeinen, M. Myllys, P. Kekäläinen and J. Timonen. Dynamic interface detection using quench Edwards-Wilkinson equation. In preparation.

[12] M.B. Priestley. Spectral analysis and time series. Vol. I and II. Academic Press (1981).

[13] N.I. Fisher. Statistical analysis of circular data. Cambridge University Press (1995).